# Relaxation Approximations to Shallow Water and Pollutant Transport Equations

**A.I. Delis**

Department of Sciences, Division of Mathematics,

Technical University of Crete, University Campus,

Chania 73100, Crete, Greece

Phone: +30- 28210- 37751, Fax: +30-28210-37842, E-mail: adelis@science.tuc.gr

and

**Th. Katsaounis**

Department of Applied Mathematics,

University of Crete,

Heraklion 71409, Crete, Greece

E-mail: thodoros@tem.uoc.gr

**Abstract - A Riemann-solver free scheme is presented for the numerical solution of shallow water flows and the transport and diffusion of pollutant in such flows. By first transforming the original nonlinear system, that governs such flows, to a semilinear system, with relaxation source and applying a non-oscillatory reconstruction and an asymptotic preserving method for space and time discritizations, numerical results are presented in one and two dimensions showing that the method can be considered as an alternative to classical finite difference methods.**

*Keywords*— **Shallow water flows, Transport of Pollutant, Relaxation Schemes**

## I. INTRODUCTION

In recent years many methods were proposed for the numerical approximation of solutions of hyperbolic conservations laws for complex applications. There has been a growing trend in favor of Riemann or Godunov-type based methods constructed within the finite volume framework. Such methods are noted for their good conservation and shock capturing capabilities. More recently many methods were proposed for the numerical approximation of solutions of hyperbolic conservations laws incorporating source terms, with application to the shallow water equations, based on such methods.

The purpose of the present work is to report on the applicability of recently developed relaxation algorithms for shallow flows, introduced in [DK 03] and [DK 05], for the solution of one and two-dimensional problems with pollutant transport. The starting point of our investigation is the class of relaxation schemes, first introduced in [JX 95], which are based on a relaxation approximation to the nonlinear conservation law, that has linear convection term and does not need a Riemann solver nor characteristic decomposition and thus enjoy great simplicity. This simplicity can be of great significance when one has to solve large scale engineering problems. Theoretical results on relaxation schemes problems have been extensively covered in the literature, these include convergence analysis, error estimates as well as nonlinear stability.

We use finite volume shock capturing spatial discretizations that are Riemann solver free, while a Runge–Kutta method provides the time stepping mechanisms. The proposed schemes combine simplicity and high efficiency. Their performance in various test problems shows that provide a reliable alternative method for wave computations in one and two dimensions. Numerical results are presented for several test problems with or without the source term present and the presented schemes are verified by comparing the results with analytical and documented ones.

## II. MODEL EQUATIONS

We depart from the well known two-dimensional shallow water (SW) system, with a geometrical source term added, written in it's physical conservative form,

$$\frac{\partial h}{\partial t} + \mathrm{div}(h\mathbf{u}) = \Sigma(\mathrm{x},\mathrm{y},\mathrm{t}), \qquad (1)$$

$$\frac{\partial h\mathbf{u}}{\partial t} + \mathrm{div}(h\mathbf{u} \otimes \mathbf{u}) + \nabla\left(\frac{\mathrm{g}}{2}\mathrm{h}^2\right) = -\mathrm{gh}\nabla\mathrm{Z} \qquad (2)$$

where we denote $h(t,x,y) \geq 0$, the water depth at time $t$, $\mathbf{u} = (u_1, u_2)^{\mathrm{T}}$, the flow velocity, $g$ the gravitational acceleration, $Z(x,y)$ the bottom topography and $\Sigma(x,y,t)$ are the sources of water. We also denote with $\mathbf{q}=h\mathbf{u}$ the water discharge.

A wide variety of physical phenomena are governed by the SW equations. An important class of problems of practical interest involve such water flows, including tidal flows in estuary and coastal water regions, bore wave propagation, flood waves in rivers, surges and dam-break modelling among others. The inclusion of source terms, e.g., those terms relevant to bottom topography is often necessary to permit the modelling of such realistic problems.

The SW system is being used to provide the hydrodynamic background for the propagation and diffusion of a passive pollutant in the water which is modeled by the equation

$$\frac{\partial hC}{\partial t} + \text{div}(h\mathbf{u}C) - \text{div}(h\mathbf{D}\nabla C) = \Sigma C_\Sigma, \qquad (3)$$

where $C(t, x, y)$) is the average pollutant concentration, $C_\Sigma$ is a given concentration of the pollutant at the sources $\Sigma$ and $\mathbf{D} = (D^x, D^y)^T$ are diffusion coefficients. Equations (1), (2) and (3) are coupled through the source terms and can be written in differential conservation law form as a single vector equation.

It is well known that the solutions of such nonlinear systems present steep fronts and shock discontinuities, which need to be resolved accurately in applications, and can cause severe numerical difficulties. Thus, computing numerical solutions is not trivial due to nonlinearity, the presence of the convective term and the coupling of the equations through the source terms.

## III. RELAXATION APPROXIMATIONS

Consider an extended (with a general source term present) nonlinear system of conservation laws in one space dimension, with initial data,

$$\frac{\partial \mathbf{u}}{\partial t} + \frac{\partial \mathbf{f}(\mathbf{u})}{\partial x} = \mathbf{s}(\mathbf{u}),$$
$$\mathbf{u}(x, 0) = \mathbf{u}_0(x), \qquad (4)$$

where the functions $\mathbf{u}$ and $\mathbf{f}(\mathbf{u}) \in R^n$. Introducing the artificial variable $\mathbf{v}$ (relaxation variable), the corresponding relaxation system is then given by

$$\frac{\partial \mathbf{u}}{\partial t} + \frac{\partial \mathbf{v}}{\partial x} = \mathbf{s}(\mathbf{u}),$$
$$\frac{\partial \mathbf{v}}{\partial t} + \mathbf{C}^2 \frac{\partial \mathbf{u}}{\partial x} = -\frac{1}{\epsilon}(\mathbf{v} - \mathbf{f}(\mathbf{u})), \qquad (5)$$

with initial data

$$\mathbf{u}(x, 0) = \mathbf{u}_0(x),$$
$$\mathbf{v}(x, 0) = \mathbf{v}_0(x) = \mathbf{f}(\mathbf{u}_0(x)),$$

where the small parameter $\epsilon$ is the *relaxation rate* ($0 < \epsilon \ll 1$) and

$$\mathbf{C}^2 = \text{diag}\{c_1^2, c_2^2, \dots, c_n^2\}$$

is a positive diagonal matrix to be chosen. Here we must require that the well-known *sub-characteristic condition* holds given by

$$\mathbf{C}^2 - \mathbf{f}'(\mathbf{u})^2 \geq 0, \quad \forall \mathbf{u}. \qquad (6)$$

This condition ensures the dissipative nature of the approximation. Hence, for the one-dimensional case we require that every eigenvalue $\lambda_i$ of $\mathbf{f}'(\mathbf{u})$ satisfies

$$|\lambda| \leq c_{\max}, \qquad (7)$$

where $c_{\max} = \max_i c_i$. By doing so we insure that the characteristic speeds of the hyperbolic part of (5) are at least as large as the characteristic speeds of the original problem. Consequently, in the limit $\epsilon \rightarrow 0^+$ system (5) approaches the original system (5) by the *local equilibrium* $\mathbf{v} = \mathbf{f}(\mathbf{u})$.

Following the previous motivation we write a relaxation system for the 1D equations replacing the conservation laws (1)-(3) by a larger system

$$\frac{\partial \mathbf{w}}{\partial t} + \frac{\partial \mathbf{H}(\mathbf{w})}{\partial x} = \mathbf{B}(\mathbf{w}), \qquad (8)$$

where $\mathbf{w}, \mathbf{H}$, and $\mathbf{B} \in R^{2n}$ and the new vectors are stated explicitly as

$$\mathbf{w} = \begin{pmatrix} u_1 \\ \vdots \\ u_n \\ v_1 \\ \vdots \\ v_n \end{pmatrix}, \mathbf{H} = \begin{pmatrix} v_1 \\ \vdots \\ v_n \\ c_1^2 u_1 \\ \vdots \\ c_n^2 u_n \end{pmatrix}, \mathbf{B} = \begin{pmatrix} s_1 \\ \vdots \\ s_n \\ -\frac{1}{\epsilon}(v_1 - f_1) \\ \vdots \\ -\frac{1}{\epsilon}(v_n - f_n) \end{pmatrix}.$$

We can see now that system (1)-(3) can be easily converted to the relaxation system (8) in a straightforward manner. We should note here that the characteristic variables are still much simpler than those of the non-linear conservation law, since the relaxation system has linear characteristic variables, and that no information about the eigensystem of the Jacobian of the nonlinear flux is required, except an upper bound of the largest eigenvalue in modulus, in order to adjust the parameters in $\mathbf{C}^2$ according to the subcharacteristic condition. We note that for the hyperbolic system (1)-(3), and for the 1D case, the eigenvalues of the Jacobian are $\lambda_{1,2} = u \pm \sqrt{gh}, \lambda_3 = u$.

Next we present the semi-discrete relaxation schemes for the larger system where we consider possible spatial discretizations. To discretize the system of equations (8) we assume a uniform spaced grid with $\Delta x = x_{i+\frac{1}{2}} - x_{i-\frac{1}{2}}$ and a variable time step (calculated based on a CFL condition) $\Delta t = t^{n+1} - t^n$, $n = 0, 1, 2, \dots$. The approximate

solution, denoted as the discrete value $\mathbf{w}_i^n$, is the approximate cell average of the variable $\mathbf{w}$ in the cell $(x_{i+\frac{1}{2}}, x_{i-\frac{1}{2}})$ at time $t = t^n$. The approximate point value of $\mathbf{w}$ at $x = x_{i+\frac{1}{2}}$ at time $t = t^n$ is denoted by $\mathbf{w}_{i+\frac{1}{2}}^n$. We then

construct a classical first order in space upwind scheme and a second order MUSCL-type scheme, and present the time discretization of the relaxation scheme applied to the equations. We present a MUSCL-TVD space discretization, and a Runge-Kutta method as the time marching mechanism to advance the solution in time, which reads as

$$\mathbf{w}^{n,1} = \mathbf{w}^n + \Delta t \mathbf{B}(\mathbf{w}^{n,1}), \tag{9a}$$

$$\mathbf{w}^{(1)} = \mathbf{w}^{n,1} - \Delta t D_+ \mathbf{H}(\mathbf{w}^{n,1}), \tag{9b}$$

$$\mathbf{w}^{n,2} = \mathbf{w}^{(1)} - \Delta t \mathbf{B}(\mathbf{w}^{n,2}) - 2\Delta t \mathbf{B}(\mathbf{w}^{n,1}) \tag{9c}$$

$$\mathbf{w}^{(2)} = \mathbf{w}^{n,2} - \Delta t D_+ \mathbf{H}(\mathbf{w}^{n,2}) \tag{9d}$$

$$\mathbf{w}^{n+1} = \frac{1}{2}(\mathbf{w}^n + \mathbf{w}^{(2)}). \tag{9e}$$

This second order implicit-explicit (IMEX) Runge-Kutta splitting scheme utilized here is different to the one presented for the shallow water equations in [DK 05]. For the first $n$ components of $\mathbf{w}$ in equations (11a) and (11c) one does not have to solve any implicit problems due to the special structure of the source term in equation (3) (following from (1)), while for the second $n$ components one can again solve explicitly (that due to linearity of $\mathbf{v}$). For example, for the first $n$ components of $\mathbf{w}^{n,1}$ in equation (11a) we have

$$u_i^{n,1} = u_i^n - \Delta t s_i(\mathbf{u}_i^{n,1}), \tag{10}$$

while for the second $n$ components we have

$$v_i^{n,1} = v_i^n - \frac{\Delta t}{\epsilon}\left[f_i(\mathbf{u}_i^{n,1}) - v_i^{n,1}\right], \tag{11}$$

which we solve explicitly as

$$v_i^{n,1} = \frac{\left[v_i^n - \frac{\Delta t}{\epsilon}f_i(\mathbf{u}_i^{n,1})\right]}{\left(1 - \frac{\Delta t}{\epsilon}\right)}. \tag{12}$$

Hence, this splitting treats, alternatively, the stiff source terms $\frac{1}{\epsilon}(\mathbf{v} - \mathbf{f}(\mathbf{u}))$ implicitly in two steps (that due to the structure of the source terms and the linearity of $\mathbf{v}$ one still solve them explicitly), and the convection terms with two explicit steps. Thus, we have an explicit implementation of an implicit source term, with stability constraints solely determined by the non-stiff convection terms, just as in a usual shock capturing scheme.

The spatial discretization is introduced in (9) by the operator

$$D_+ \mathbf{H} = \frac{1}{\Delta x}(\mathbf{H}_{i+\frac{1}{2}} - \mathbf{H}_{i-\frac{1}{2}}).$$

To solve for $\mathbf{H}_{i\pm\frac{1}{2}}$ and construct a second order accurate in space scheme, the MUSCL-TVD piecewise linear interpolation is applied to the $k-$th component of $\mathbf{v} \pm \mathbf{Cu}$, gives respectively:

$$(v + c_k u)_{i+\frac{1}{2}} = (v + c_k u)_i + \frac{1}{2}\Delta x \sigma_i^+,$$

$$(v - c_k u)_{i+\frac{1}{2}} = (v - c_k u)_{i+1} - \frac{1}{2}\Delta x \sigma_{i+1}^-, \tag{13}$$

where $u, v$ are the $k-$th ($1 \le k \le n$) components of $\mathbf{v}, \mathbf{u}$ respectively, with $\sigma$ the slopes in the $i-$th cell defined as

$$\sigma_i^\pm = \frac{1}{\Delta x}(v_{i+1} \pm c_k u_{i+1} - v_i \mp c_k u_i)\phi(\theta_i^\pm) \tag{14}$$

and

$$\theta_i^\pm = \frac{v_i \pm c_k u_i - v_{i-1} \mp c_k u_{i-1}}{v_{i+1} \pm c_k u_{i+1} - v_i \mp c_k u_i}, \tag{15}$$

where $\phi$ is a *limiter* function, satisfying

$$0 \le \phi(\theta) \le \text{minmod}(2, 2\theta). \tag{16}$$

There are several options on choosing a limiter function. Some of the most popular ones are, the MinMod (MM) limiter

$$\phi(\theta) = \max(0, \min(1, \theta)),$$

the VanLeer (VL) limiter

$$\phi(\theta) = \frac{|\theta| + \theta}{1 + |\theta|},$$

the Superbee (SB) limiter

$$\phi(\theta) = \max(0, \min(2\theta, 1), \min(\theta, 2)),$$

and the Monotonized Central (MC) limiter

$$\phi(\theta) = \max(0, \min((1 + \theta)/2, 2, 2\theta)).$$

Following from (13) we get

$$u_{i+\frac{1}{2}} = \frac{1}{2}(u_i + u_{i+1}) - \frac{1}{2c_k}(v_{i+1} - v_i) + \frac{\Delta x}{4c_k}(\sigma_i^+ + \sigma_{i+1}^-),$$

$$v_{i+\frac{1}{2}} = \frac{1}{2}(v_i + v_{i+1} - \frac{c_k}{2}(u_{i+1} - u_i) + \frac{\Delta x}{4}(\sigma_i^+ - \sigma_{i+1}^-).$$

$$\tag{17}$$

slope $\sigma^{\pm} = 0$ or $\phi = 0$, the MUSCL scheme reduces to a *first order upwind* scheme.

It is worth noting here that, using the above schemes neither linear algebraic equation nor nonlinear source terms arise. In addition both first and second order relaxation schemes are stable under a *CFL* condition

$$\max\left((\max_i c_i)\frac{\Delta t}{\Delta x}\right) \leq 1. \qquad (18)$$

In order to retain the TVD property (see [JX 95]) a more strict restriction has to be imposed on the usual *CFL* condition, and that has been applied in the following section n in order to calculate $\Delta t$

$$CFL = \max\left((\max_i c_i)\frac{\Delta t}{\Delta x}\right) \leq \frac{1}{2}. \qquad (19)$$

It is worth noting that, using the above scheme neither linear algebraic equations nor nonlinear source terms arise. In addition this second order relaxation scheme is stable and non-oscillatory under the $CFL$ condition.

### IV. 1D NUMERICAL TESTS AND RESULTS

We present results of a series of numerical experiments illustrating the various features of the schemes. For consistency in all the experiments reported here the time step $\Delta t$ was computed according to the condition (18), but in practice higher values can also be used in most calculations.

The choices of $c_i$ in all the numerical tests are based on rough estimates of the eigenvalues ($u + \sqrt{gh}, u - \sqrt{gh}, u$) of the original (1)–(3) equations. Thus, we take $c_i \geq \sup|\lambda_i|$ which satisfy the subcharacteristic condition (7). Other choices can be made, for example one can simply set $c_i = \max(\sup|\lambda_i|)\forall i$, as long as numerical stability is maintained. It should be noted here that larger $c_i$ values usually add more numerical viscosity. The schemes presented here can be viewed as a whole class of schemes depending on the parameters $c_i$.

The relaxation parameter $\epsilon$ should be small with respect to the time step and space mesh length, that is $\Delta t \gg \epsilon$ and $\Delta x \gg \epsilon$. Again here, $\epsilon$ plays the role of viscosity coefficient so more numerical diffusion will be added for relatively larger values of $\epsilon$

#### A. 1D Dam-Break Problem

The first test case is of a dam break on a flat bottom, where the concentration of the pollutant has different values on each side of the dam. We compare the results with exact solutions (presented as solid lines). For this first problem the channel length is $L = 50m$. The initial data is that of a Riemann problem, with $x_0 = 10m$ being the dam position (position of the initial discontinuity). The values $h_L = 1m, u_L = 2.5m/s$ and $C_L = 1$ are the initial value at the left side of the dam, with right values $h_R = 0.1m, u_R = 0m/s$ and $C_R = 0$. The simulation time is $t_{out} = 7s$. Figures (1)-(3) show the results for water height, water discharge and pollutant concentration obtained with the relaxation scheme with computational parameters $\Delta x = 0.5m, \epsilon = 1.D - 6, c_1 = 6.5, c_2 = 1.4$ and $c_3 = 4$. The VL limiter was used to obtain these results. We are particularly interested in the performance of the scheme for the pollutant concentration. The numerical solution closely follows the exact one, with the pollutant shock front well captured for the coarse grid used.

#### B. Emission of Pollutant Over Topography

This test case is also from [AB 03]. Here we test the introduction of a source of pollutant is a flow. For this problem the initial data is $h + Z = 2$, $q = 0.5$ with $L = 1000m$ and $g = 1$ with

$$Z(x) = \begin{cases} 0.2 - 0.05(x - 10)^2, & 8 \leq x \leq 12, \\ 0, & \text{otherwise.} \end{cases}$$

We assume that the water is initially clean until time $t_b = 100s$ (where the flow has reached a steady state at this point) when a source of water $\Sigma = 0.01$ with concentration of pollutant $C_\Sigma = 10$ is turned on at the point $x = 45m$, then at time $t_e = 300s$ the pollution source is turned off. Then we follow the evolution of this pollutant layer.

Using $\Delta x = 4m, \epsilon = 1.D - 6, c_1 = 2, c_2 = 1$ and $c_3 = 0.5$ with the MC limiter, numerical results for the pollutant concentration are presented in Figures (4) and (5) at times $t_{out} = 300s, 350s, 500s$ and $800s$, for the interval $I = [0, 500]$. The results are in very good agreement with those presented in [AB 03], [KCP 05]. As pointed out in [AB 03] due to the presence of the water source there is a local modification in space and time of the hydrodynamic computation. Here we prove that the relaxation scheme can cope with such situations producing reliable results.

### V. 2D NUMERICAL TESTS AND RESULTS

In this section we apply the relaxation scheme to two-dimensional problems. We will not make a complete presentation of the extension of the scheme in 2D here, since it will be detailed elsewhere. The 2D computations are based on extending the 1D strategy.

We will just present the 2D relaxation model that corresponds to equation (5) for the 1D case. Considering the
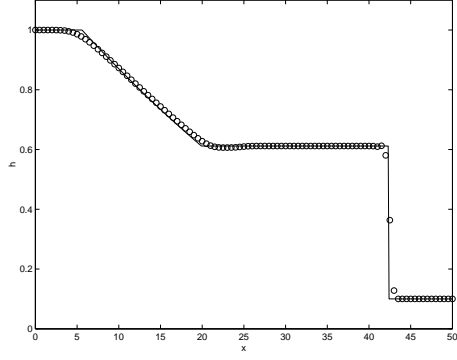
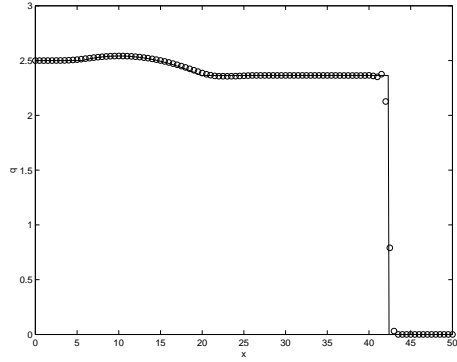Fig. 1. Dam Break problem: water height at $t_{out}$=7s. Exact solution (–) and MUSCL (o–).



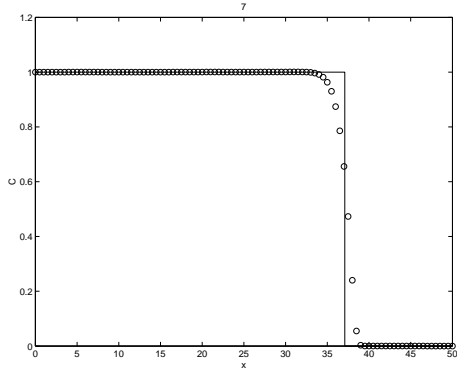Fig. 2. Dam Break problem: water discharge at $t_{out}$=7s. Exact solution (–) and MUSCL (o–).



Fig. 3. Dam Break problem: pollutant concentration at $t_{out}$=7s. Exact solution (–) and MUSCL (o–).
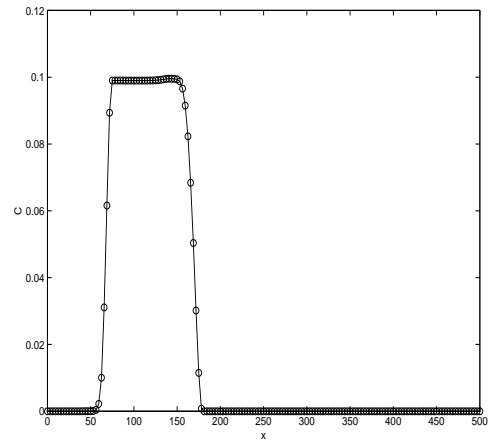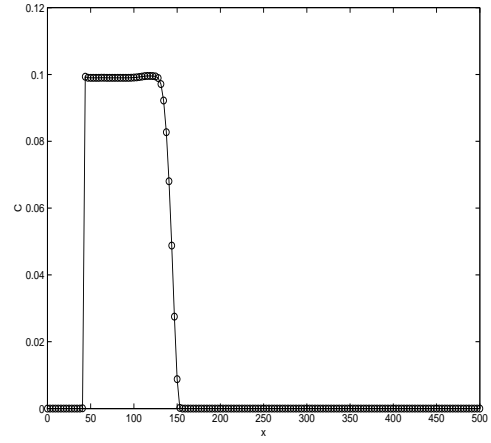


Fig. 4. Emission of Pollutant Over Topography: concentration of the pollutant at times $t = 300s$ (left) and $t = 350s$ (right) for the MUSCL relaxation scheme.

classical 2-D conservation law

$$\frac{\partial \mathbf{u}}{\partial t} + \frac{\partial \mathbf{f}(\mathbf{u})}{\partial x} + \frac{\partial \mathbf{g}(\mathbf{u})}{\partial y} = \mathbf{s}(\mathbf{u}); \quad (x, y) \in R^2, \ t > 0,$$

$$\mathbf{u}(x, y, 0) = \mathbf{u}_0(x, y); \quad (x, y) \in R^2$$

(20)

with $\mathbf{u}, \mathbf{f}(\mathbf{u})$ and $\mathbf{g}(\mathbf{u}) \in R^n$ we introduce the relaxation variables $\mathbf{v}, \mathbf{w}$ to (20), and the linear relaxation model in 2D reads as follows,

$$\frac{\partial \mathbf{u}}{\partial t} + \frac{\partial \mathbf{v}}{\partial x} + \frac{\partial \mathbf{w}}{\partial y} = \mathbf{s}(\mathbf{u}),$$

$$\frac{\partial \mathbf{v}}{\partial t} + \mathbf{C}^2 \frac{\partial \mathbf{u}}{\partial x} = -\frac{1}{\epsilon}(\mathbf{v} - \mathbf{F}(\mathbf{u})) \qquad (21)$$

$$\frac{\partial \mathbf{w}}{\partial t} + \mathbf{D}^2 \frac{\partial \mathbf{u}}{\partial y} = -\frac{1}{\epsilon}(\mathbf{w} - \mathbf{G}(\mathbf{u})),$$

where now $\mathbf{C}^2, \mathbf{D}^2 \in R^{n \times n}$ are positive diagonal matrices. In the limit $\epsilon \to 0^+$ system (21) approaches the original system (2.1) by the *local equilibrium* $\mathbf{v} = \mathbf{F}(\mathbf{u})$ and $\mathbf{w} = \mathbf{G}(\mathbf{u})$. A general necessary condition for such convergence is that a sub-characteristic like condition is satisfied. For system (21) we require that,

$$\frac{\lambda_i^2}{c_i^2} + \frac{\mu_i^2}{d_i^2} \leq 1, \quad \forall i \qquad (22)$$
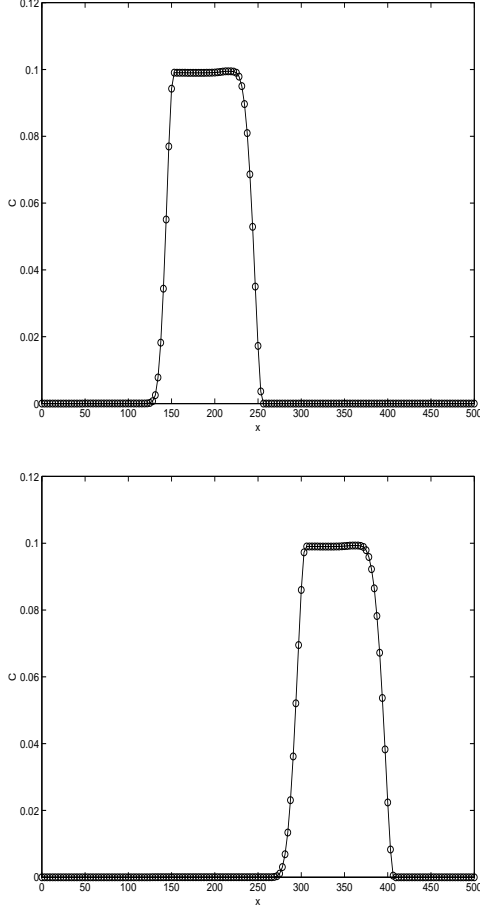
Fig. 5. Emission of Pollutant Over Topography: concentration of the pollutant at times $t = 500s$ (left) and $t = 800s$ (right) for the MUSCL relaxation scheme.

with $\lambda_i, \mu_i$ being the eigenvalues of $\partial \mathbf{F(u)}/\partial \mathbf{u}$ and $\partial \mathbf{G(u)}/\partial \mathbf{u}$ respectively.

### A. A 2D Partial Dam-Break

This problem is similar to the one considered in [CK 05] and is the case of a 2D square domain $1400m \times 1400m$ where the water flows through a breach that is located between $y = 560$ and $y = 840$, from the left to the right. The initial data is $u_L = u_R = v_L = v_R = 0$ and $h_L = 0.5m$ and $h_R = 1m$. The initial pollutant concentration is given by $C(x,y,0) = e^{-0.0001[(x-650)^2+(y-600)^2]}$ for $0 \leq x \leq 700, 0 \leq y \leq 1400$ and $C(x,y,0) = 0.5$ for $700 \leq x \leq 1400, 0 \leq y \leq 1400$. The boundary conditions at $x = 0$ and $x = 1400m$ are assumed to be transmissive and all other boundaries are considered as reflective. At the instant of breaking of the dam, water is released through the breach, forming a positive wave propagating downstream and a negative wave spreading upstream. The computational parameters used were $\epsilon = 10^{-6}$ and $c_1 = 10, c_2 = 6, c_3 = 11, d_1 = 10, d_2 = 5, d_3 = 11$. The VL limiter was applied in all computations. The solu-

tion computed on a $500 \times 500$ grid at time $t_{out} = 200s$ is shown in Figures (V-A) and (V-A). The scheme provides a very high resolution of circular shock wave and the vortices formed on the breach. The results for the pollutant concentration correctly describe the physical behavior and are comparable to those presented in [CK 05].
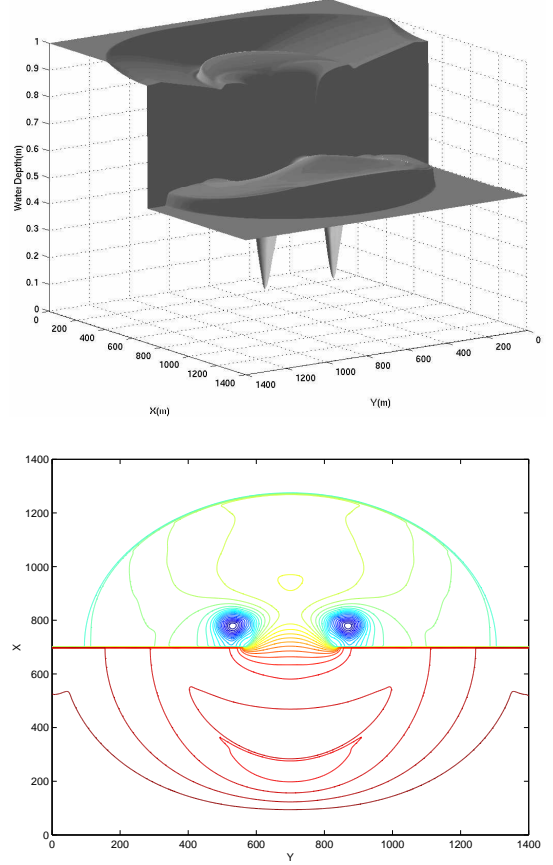




Fig. 6. A 2D Partial Dam Break: 3D plot (top) and contour plot (bottom) for water height at $t_{out} = 200s$ computed with the MUSCL relaxation scheme.

### B. Emission of Pollutant in a Reservoir

This test problem is to simulate the transport and diffusion in a reservoir. The computational domain is a $200m \times 200m$ region which has been subdivided into $81 \times 81$ square grid. The initial stagnant water depth in the reservoir is $h = h_L = 1m = h_R$ and $u_1 = u_2 = 0$, with no pollutant present inside the domain. The values of the diffusion coefficients are $D_x = D_y = 29.2m^2/s$ A breach exists, located in the middle of the reservoir, and is $75m$ in length, having distances of 30m from the left bank and 95m from the right. The boundary conditions at $x = 0$ and $x = 200m$ are assumed to be transmissive and all other boundaries are considered as reflective. At the beginning at the inlet of the reservoir we impose $u_1 = 0.1m/s$ and a pollutant is released with $C = 0.7$. The computational parameters used were $\epsilon = 1.D - 6$ and $c_1 = c_3 = 4, c_2 = c_4 = 0.25, d_1 = d_3 = 4, d_2 = d_4 = 0.15$, with the MC limiter.
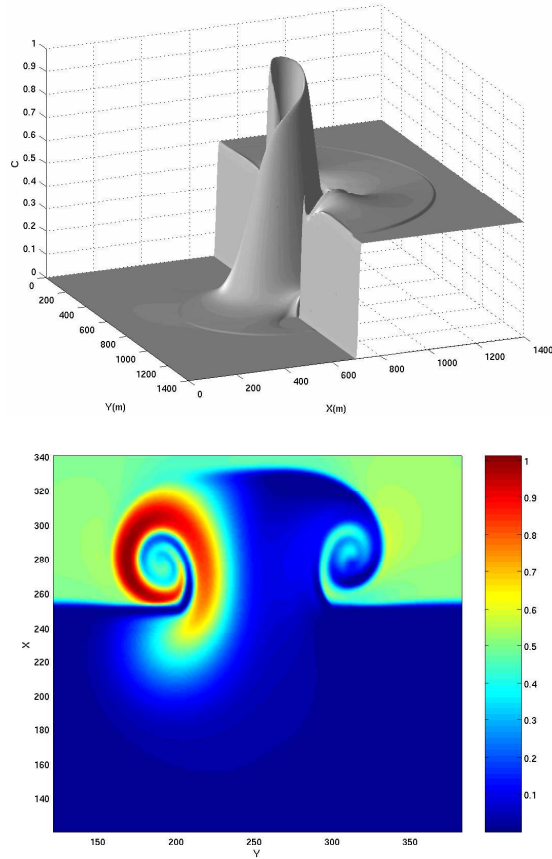
Fig. 7. A 2D Partial Dam Break: 3D plot (top) and magnified top view (bottom) for the pollutant concentration $t_{out} = 200s$ computed with the MUSCL relaxation scheme.
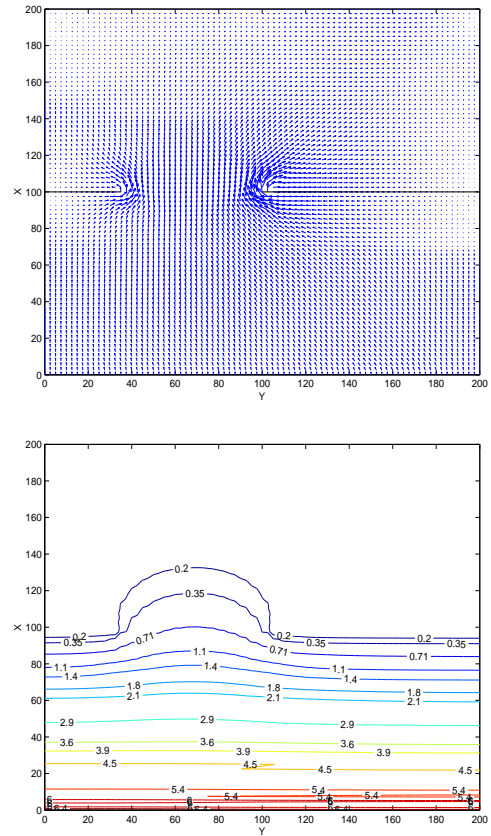
Fig. 8. Emission of pollutant in a reservoir: velocity field (left) and pollutant concentration contours (right) at time $t = 80s$ computed with the MUSCL relaxation scheme.

The results for two consecutive representations in terms of velocity fields and pollutant concentration distribution are presented in Figure (8). We can clearly see the discharge effect to the evolution of the pollutant concentration on the initially stagnant reservoir water.

## VI. CONCLUSIONS

In the present work relaxation schemes have been studied in order to compute numerical solutions for the two dimensional shallow water flows along with transport and diffusion of pollutant in such flows. The main feature of the schemes is their simplicity and robustness. Finite volume shock capturing spatial discretization, that are Riemann solver free, have been used providing accurate shock resolution.The schemes has been extended in two dimensions. The benchmark tests have shown that the schemes provide accurate solutions in good agreement with analytical or reference solutions. The results also demonstrate that relaxation schemes are accurate, simple, efficient and robust and can be of practical consideration and further study. Further possible developments of the method can be considered, like higher order spatial discretizations, different Runge-Kutta time stepping methods and an adaptive way

of calculating the characteristic speeds. These are interesting areas of numerical analysis that can benefit from further investigation.

## REFERENCES

[AB 03] E. Audusse and M. O. Bristeau, *Transport of pollutant in shallow water. A two time steps kinetic method*, M2AN Math. Model. Numer. Anal., **37** (2003), pp. 389–416.

[KCP 05] A. Chertock, A. Kurganov and G. Petrova, *Finite Volume Particle Methods for Models of Transport of Pollutant is Shallow Water*, (to appear in) J. Sci. Comput, (2005)

[CK 05] A. Chertock and A. Kurganov, *On a Hybrid Finite-Volume-Particle Method*, (to appear in) M2AN Math. Model. Numer. Anal., (2005)

[DK 03] A.I. Delis and Th. Katsaounis, *Relaxation schemes for the shallow water equations*, Int. J. for Numerical Meth. in Fluids, **41** (2003), pp. 695–719.

[DK 05] A.I. Delis and Th. Katsaounis, *Numerical solution of the two-dimensional shallow water equations by the application of relaxation methods*, Applied Mathematical Modelling (to appear), 2005.

[JX 95] S. Jin and Z. Xin, *The relaxing schemes of conservations laws in arbitrary space dimensions*, Comm. Pure Appl. Math, **48** (1995), pp. 235–277.